



**AIAA 2000–4230**

**Flutter Predictions by a Filtered  
Impulse Method**

Feng Liu, Jinsheng Cai  
*University of California, Irvine, CA 92697-3975*

Her-Mann Tsai  
*DSO National Laboratories, Singapore 118230*

**18th AIAA Applied Aerodynamics  
Conference**

**14–17 August 2000 / Denver, CO**

# Flutter Predictions by a Filtered Impulse Method

Feng Liu\*, Jinsheng Cai†

*University of California, Irvine, CA 92697-3975*

Her-Mann Tsai‡

*DSO National Laboratories, Singapore 118230*

The indicial response method is a fast tool for calculating the dynamic response of an aerodynamic system that can be used for flutter predictions based on methods on the frequency domain. The conventional way of calculating the indicial response by using a step function or impulse function inputs has difficulties in practical application when a CFD method is used to calculate the response because of the non-smooth nature of the input functions. Three input functions that avoid potential non-physical responses while at the same time provides adequate resolution for frequencies of interest of a given aeroelastic system are studied with a model dynamic system and a two-dimensional wing model. The important parameters for accuracy and efficiency in the numerical calculation of the frequency response by the indicial method are discussed. Guidance is given on the choice of time step size and integration length as well as the effect of the power spectrum of the input functions.

## I. Nomenclature

$c$	airfoil chord length.
$U_\infty$	freestream velocity.
$\omega_\alpha$	lowest angular frequency of interest.
$\omega$	dimensionless angular frequency based on $\omega_\alpha$ .
$\kappa$	reduced frequency, $\omega c/2U_\infty$ .
$t$	dimensionless time based on $1/\omega_\alpha$ .
$f(t)$	input signal.
$\mathcal{F}(f(t))$	Fourier transform of $f(t)$ .
$q_{ij}(t)$	response of the generalized aerodynamic force on mode $i$ due to motion of mode $j$ .
$A_{ij}(\kappa)$	transfer function for the generalized aerodynamic force $q_{ij}$ , $\mathcal{F}(q_{ij}(t))/\mathcal{F}(f(t))$ .
$I$	unit imaginary number, $\sqrt{-1}$ .

## II. Introduction

Time accurate solution with the coupled Euler/Navier-Stokes equations and the structural modal equations provides a powerful tool for simulating aerodynamic flutter phenomena.<sup>1-3</sup> However, the method is rather time consuming when used for the purpose of predicting the onset of flutter since many “brute-force” runs have to be performed

in order to locate the flutter boundary for a given aerodynamic/structure system.

For engineering purposes, a more efficient, albeit more restrictive, method is to obtain the Generalized Aerodynamic Force (GAF) by performing the aerodynamic calculations off-line (decoupled with the structural dynamic equations), and then feeding the GAF to the structural equations to perform a classical root-loci analysis in order to obtain the stability boundary of the structural system. For this purpose, the General Aerodynamic Force (GAF) matrix must be obtained for each input frequency  $\omega$ . Although, this method is restricted to linear structural systems and the aerodynamic response around the mean flow is assumed to be linear too, the mean flow itself is not limited to a linear solution.

There are two methods to obtain the GAF matrix. The first being the traditional harmonic method, in which a sinusoidal input of a given frequency of each structural mode is fed into the flow code. The flow solver (Euler/Navier-Stokes) is used to integrate the flow equations in time for several periods until the system reaches a periodic motion, at which time the aerodynamic forces on the wing are integrated over the last period of the computation. A Fourier transform is then performed on the aerodynamic forces to obtain the GAF matrix  $A_{ij}$  on the complex domain. A series of such computations must be performed in order to get the GAF matrix,  $A_{ij}(\kappa)$ , for a range of frequencies of interest and for each mode of the structural system.

The harmonic method is a rather time-consuming method. An alternative is to use the Indicial Method originally proposed by Tobak,<sup>4</sup> and also by Ballhaus and Goorjian,<sup>5</sup> in which, a step function input excita-

Copyright © 2000 by the authors. Published by the American Institute of Aeronautics and Astronautics, Inc. with permission.

\*Associate Professor of Mechanical and Aerospace Engineering, Senior member AIAA.

†Visiting Research Specialist, Department of Mechanical and Aerospace Engineering; currently Associate Professor, Department of Astronautics, Northwestern Polytechnical University, Xi'an 710036, China.

‡Senior Member of Technical Staff, 20 Science Park Drive; currently Adjunct Associate Professor, Temasek Laboratories, National University of Singapore, Singapore 119260, Republic of Singapore. Member AIAA;

tion is fed into the aerodynamic system for each structural mode. The response of the aerodynamics system is called the Indicial Response. A Fourier analysis on this Indicial Response is enough to deduce the system response  $A_{ij}(\kappa)$  for the complete range of  $\kappa$ . In this way, only one time-integration of the Euler/Navier-Stokes is needed for each mode of the structural system in order to obtain the complete GAF matrix  $A_{ij}(\kappa)$ .

Unfortunately, the discontinuous step input proposed by Ballhaus and Goorjian<sup>5</sup> causes potential non-physical responses in a CFD simulation on the time domain due to the use of Dirac delta function associated with the derivative of the step function at  $t = 0$ . In addition, numerical difficulties exist in both accuracy and efficiency in resolving the step function response. Since all information is concentrated in the step function, very fine time steps have to be used in order to resolve the high frequency contents. On the other hand, the system relaxes after the initial step input over a long time. Therefore, computations have to be performed over a rather long time period in order to capture the low frequency response of the system. This causes long computational time and compromised accuracy in the calculated aerodynamic response.

Seidel, Bennett and Ricketts<sup>6</sup> introduced a impulse function method in which they used a non-discontinuous impulse function as the input. The impulse (IM) function is defined as

$$f(t) = e^{-W(t-t_c)^2} \quad (1)$$

where  $W$  controls the width of the impulse, and  $t_c$  is a time delay for the center of the impulse. Because the impulse function and its derivative are continuous, the impulse function method reduces the potential of non-physical responses and the numerical difficulties of the step function method. However, in practice, the accuracy and the efficiency of the method depends on the choice of  $W$ . Larger values of  $W$  gives better accuracy for high frequencies but compromises the accuracy at low frequencies. Furthermore, the choices of numerical time step size and integration length in time are of key importance to the accuracy of the numerical computation.

In this paper, we propose and evaluate the efficiency and accuracy of a new filtered impulse method based on the idea of “selected frequencies of interest”. We use input functions that are smooth but provide enhanced resolution for frequencies in the neighborhood of the structural frequencies of the aeroelastic system. One particular filtered impulse function is found to reduce computational time while maintaining accuracy both at the low and the high frequency range compared to the the impulse function (1). The key parameters that affect the accuracy and efficiency in calculating the frequency response of an aerodynamic system using an implicit time marching scheme are identified. The GAF matrix  $A_{ij}(\kappa)$  obtained in this

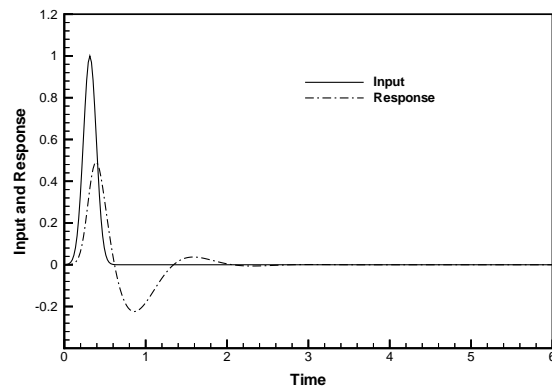


**Fig. 1** The IM function (1) for  $W = 80$ ,  $t_c = \pi/10$  and response to it of the model dynamic system.

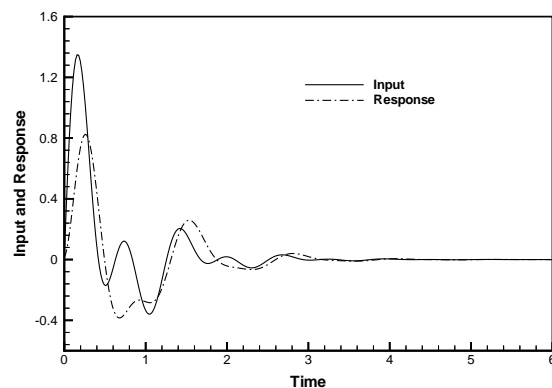


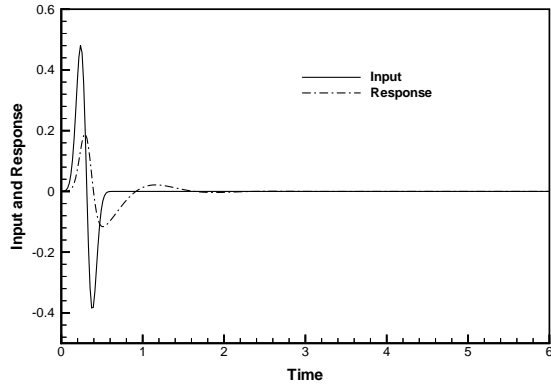
**Fig. 2** FIM function (2) and the response to it of the model dynamic system.

analysis is fed into a flutter analysis code using the V-g method to obtain the flutter boundary of the aerodynamic/structure system of an oscillating airfoil with two degrees of freedom.

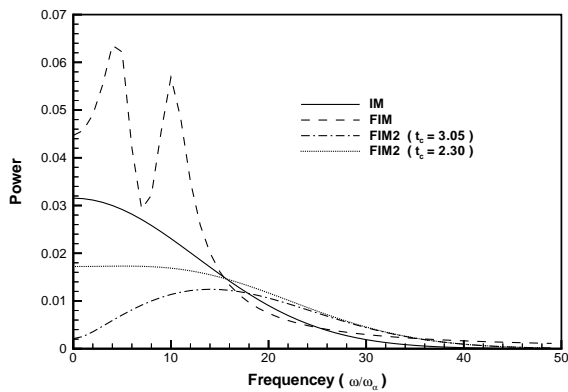
### III. The Filtered Impulse Method

Figure 1 plots the impulse function given by Equation (1) for a typical value of  $W = 80$  and  $t_c = \pi/10$  over the time from 0 to  $2\pi$ . Since  $t$  is nondimensionalized by  $1/\omega_\alpha$ , where  $\omega_\alpha$  is taken to be the lowest eigen frequency of the elastic system, the time interval  $2\pi$  stands for the longest period for all the eigen frequencies.

Figure 4 shows its power spectrum density versus the frequency  $\omega$ . Clearly, the impulse function (1) concentrates most of its energy near zero frequency. If the highest eigen frequency is 20 times of  $\omega_\alpha$ , the energy spectrum of Equation (1) shows a reduced level at this high frequency  $\omega = 20$ , indicating potential inaccuracies in the transfer function at the high frequency end. The power level at high frequencies can be increased by increasing  $W$ , thus reducing the width of the impulse. This, however, would increase the gradient of



**Fig. 3 FIM2 function (3) and the response to it of the model dynamic system.**



**Fig. 4 Power spectrum of the three different input functions.**

the function and decrease the number of grid points within the pulse if a fixed  $\Delta t$  is used.

The conventional V-g method for flutter analysis requires accurate frequency-domain aerodynamics only near certain distinct frequencies where flutter is likely to happen. This is to say that when transforming the time-domain solution to the frequency domain, the accuracy is desired only near those selected frequencies of interest. P.C. Chen<sup>7</sup> proposed the following “filtered impulse” (FIM) input function

$$f(t) = \sum_{j=1}^n e^{-at} \sin \omega_j t \quad (2)$$

where  $a$  represents the decay rate of  $f(t)$ ,  $n$  is the number of the distinct frequencies of interest, and  $\omega_j$  stands for the selected frequencies.

Figure 2 shows the above function for  $a = 1.5$ ,  $n = 2$ , and  $\omega_1 = 5$  and  $\omega_2 = 10$ . It is to be noticed that an exact transform of the FIM function exists

$$\mathcal{F}(\omega) = \sum_{j=1}^n \frac{\omega_j}{(i\omega + a)^2 + \omega_j^2}$$

The power spectrum of the FIM function is also shown in Figure 4. Unlike the impulse function given by Equation (1), the FIM function concentrates energy near the given frequencies of interest  $\omega_1$  and  $\omega_2$ . Therefore, good accuracy is expected at and near these frequencies.

A new filtered impulse function, which is called the FIM2 function for convenience, is proposed in this paper. This is written as

$$f(t) = e^{-a\omega_c^2(t-t_c/\omega_c)^2} \sin \omega_c t \quad (3)$$

Figure 3 shows this function (solid line) when  $a = 0.8$ ,  $t_c = 3.05$  and  $\omega_c = 10$ .

The FIM2 function can be viewed as the product of the original impulse function (1) multiplied by  $\sin \omega_c t$ , where  $\omega_c$  is a ‘cut-off’ frequency taken to be the highest frequency of interest. The exponential term is essentially a window function whose width is approximately one period of the cut-off frequency. If  $t_c = \pi$ , the window is exactly centered at the middle of the first period of the cut-off frequency. When this happens, the symmetry of the function will lead to almost zero power at zero frequency. If that is not desired,  $t_c$  is can be slightly perturbed from  $\pi$ . In this paper,  $t_c = 3.05$ .

The power spectrum of the new function is also shown in Figure 4 and compared with those of the IM and FIM functions. The significant features of this new function are (1) unlike the FIM function, the new function is only non-zero in one period of the cut-off frequency; (2) unlike the original impulse function, whose power is maximum at zero frequency, the new function concentrates energy near the specified cut-off frequency  $\omega_c$ ; This means that the FIM2 functions has much lower frequency contents. (3) The FIM2 function automatically adjusts its width and time delay based on one single input, i.e.,  $\omega_c$  which can be viewed as a cut-off frequency or frequency of importance. (4) If fine tuning of the power spectrum near the origin is needed, the parameter  $t_c$  may be adjusted. The further  $t_c$  is perturbed from  $\pi$ , the flatter the spectrum will be near the origin. Figure 4 also shows a case when  $t_c = 2.30$ , for which the power spectrum is almost flat from zero to the specified  $\omega_c$ .

In the following sections, we will present and analyze test results of the above three input functions on a model linear system and an actual aerodynamic system. The important parameters for accuracy and efficiency in the numerical calculation of the frequency response by the indicial method will be discussed. Analysis will be given on the choice of time step size and integration length as well as the effect of the power spectrum of the input functions.

#### IV. A Two-dimensional Wing Model

The two-dimensional Isogai wing model,<sup>8,9</sup> Case A, shown in Figure 5 is used as a ‘realistic’ test case for

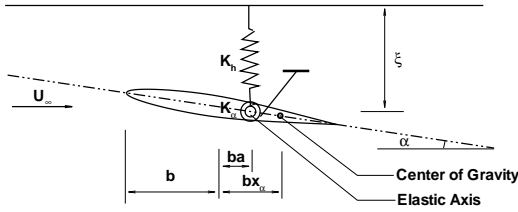


Fig. 5 The Isogai wing model

flutter calculations. This model simulates the bending and torsional motion of a wing cross-section in the outboard portion of a swept wing. It consists of two degrees of freedom, plunging and pitching, for a NACA 64A010 airfoil.

Modal equations are used to calculate the structural deformation under an aerodynamic forcing. For each mode  $i$ , the modal dynamic equation is written in the following form

$$\ddot{q}_i + 2\zeta_i\omega_i\dot{q}_i + \omega_i^2q_i = Q_i \quad (4)$$

where  $q_i$  is the generalized normal mode displacement,  $\zeta_i$  is the modal damping,  $\omega_i$  is the modal frequency, and  $Q_i$  is the generalized aerodynamic force. The structural displacement vector can be written as a summation of  $N$  modal shapes extracted from a full finite element analysis of the structure.

$$u_s = \sum_{i=1}^N q_i h_i \quad (5)$$

where  $h_i$  are the modal shapes. For the Isogai wing model,  $N = 2$ ,  $\omega_1 = 0.7134$ , and  $\omega_2 = 5.3377$ . The details of the structural model can be found in<sup>2</sup> as well as in<sup>8</sup> and<sup>9</sup>.

A multi-grid and multi-block flow solver for the solution of the three-dimensional unsteady compressible Euler/Navier-Stokes equations of a body in arbitrary motion and deformation using parallel computers has been developed in<sup>3</sup> and<sup>10</sup>. The equations are discretized in time by an implicit 2nd order time-accurate method. The structural equations are discretized by the same 2nd order implicit time marching algorithm. The implicit equations are then solved by using a dual-time stepping algorithm.<sup>2,11,12</sup> The flow solver has been validated for flutter calculations using a coupled CFD-CSD approach for both 2D airfoils and 3D wings<sup>3</sup> and is used in this paper to perform the time-domain responses to the input functions (1), (2), and (3). The results are then processed by an FFT code to obtain the generalized aerodynamic coefficient  $A_{ij}(\omega)$ .

## V. A Model Dynamic System

In order to quickly test the accuracy and efficiency of different input functions without doing full flow computations, a model dynamic system is constructed to replace the above aerodynamic system. This consists of a 2nd order linear system with a forcing function  $f(t)$ .

$$\ddot{\eta} + 2\zeta\omega_s\dot{\eta} + \omega_s^2\eta = af(t) + bf'(t) \quad (6)$$

where  $\omega_s$  is the resonant frequency, and  $\zeta$  is the damping of the system. For our test problem we have taken  $\omega_s = 5$  and  $\zeta = 0.5$ . When an input signal  $f(t)$  is fed into the system, the response of the system  $\eta$  is calculated by using the same 2nd order implicit time-marching algorithm as for the Euler/Navier-Stokes equations discussed in the above section. The frequency response of the system can then be obtained as

$$A = \frac{\mathcal{F}(\eta(t))}{\mathcal{F}(f(t))} \quad (7)$$

There are two advantages of using this linear modal equation for test purposes. First, computations can be performed quickly with many different choices of signals. Second, the exact frequency response of the system is known analytically, i.e.,

$$A_{exact} = \frac{a + bI}{(\omega_s^2 - \omega^2) + 2\zeta\omega_s\omega I} \quad (8)$$

## VI. Results and Discussions

The original IM function (1), the FIM function (2), and the new FIM2 function (3) are each tested as the forcing function  $f(t)$  first for the model problem (6). The responses of the system in the time domain are calculated by the 2nd order implicit time marching scheme mentioned in the last section. The frequency responses are then calculated by using Equation (7) and compared with the analytical solution (8).

The dashed lines in Figures 1, 2, and 3 are the responses of the model problem to the three input functions IM, FIM, and FIM2 (solid lines). These are obtained with 321 equally distributed grid points (320 intervals) over the time interval  $[0, 2\pi]$ . Figure 6 compares the calculated frequency responses and the analytical solution given by Equation (8). It can be seen that with 320 points, both the IM and FIM2 input functions reproduce the analytical solution almost perfectly.

The FIM function, however, results in significant errors compared to the analytical solution as shown by the dotted lines in Figure 6. The FIM function (2) has a discontinuous first derivative at time zero, which adversely affects the accuracy in the time integration of the system response. The 2nd order time marching scheme is based on a 3-step backward finite-difference scheme (see<sup>3</sup>) which requires initial conditions at two existing time levels in order to march forward to a third time level. Zero initial conditions for both  $\eta$  and

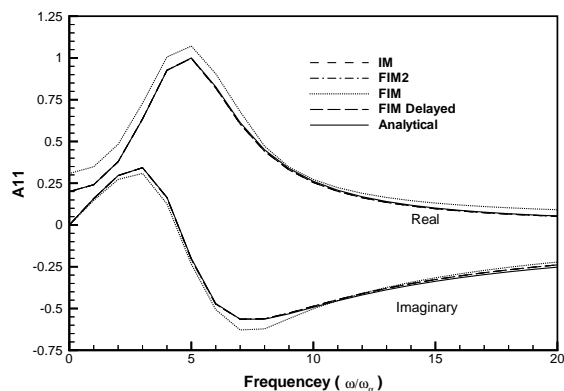


**Fig. 6** Calculated frequency responses of the model system to the IM, FIM, and FIM2, and delayed FIM inputs with 320 time steps

$\dot{\eta}$  are assumed at both  $t = 0$  and the time level before  $t = 0$ . The discontinuity in the first derivative of  $f(t)$  is particular bad when it happens at  $t = 0$  because of inaccuracies in the numerical evaluation of  $f'(t)$  and also the fact that the assumption of zero initial conditions for both  $\eta$  and  $\dot{\eta}$  are inappropriate when  $f'(t)$  is not zero. These two factors result in the errors in the frequency response calculated based on the FIM method shown as the dotted lines in Figure 6. In order to alleviate this problem, one can delay the FIM signal by a small increment in time, say 2 or 3 time steps so that the discontinuity does not happen at  $t = 0$ . With this modification, the FIM function also closely reproduces the analytical solution as shown by the dashed line marked as ‘FIM Delayed’ in Figure 6. The results shown in the rest of this paper for the FIM method all contain this modification.

Figure 6 shows that with enough grid points in time, the IM, FIM, and FIM2 functions are all capable of accurately predicting the frequency response of the model system. But how should the length of time integration and the time step size be chosen to minimize computational effort and guarantee accuracy? Is one particular input function better than others?

The accuracy and efficiency of the numerical solution depend on two factors, the total length of time for which the computations are performed and the time step size used in the time marching. In order to resolve the lowest frequency of interest,  $\omega_\alpha$ , one must cover at least one period of the said frequency in the time marching. This corresponds to a length of  $2\pi$  in our dimensionless time axis.

Within the same time period, the larger time steps one may take the less computational work one will need to do. There are three conditions that govern the maximum time step one may take.

First, Nyquist sampling principle dictates that at least two grid intervals must be used in one period of the highest frequency of interest. For example, if

the highest frequency of interest  $\omega_\beta$  is 10 times of the lowest frequency  $\omega_\alpha$ , one would then need to use at least 20 time steps within the  $2\pi$  time interval.

However, this is only the minimum number of steps needed in order to resolve the high frequency. The second condition on the time step size is accuracy. Aliasing may introduce errors in the resolved frequencies by folding the unresolved high frequency components into the resolved range. More importantly, errors are introduced in the numerical integration of the system response in the time domain. With a 2nd order finite-difference time marching scheme, the present study as well as studies in References<sup>2</sup> and<sup>12</sup> suggests that 32 time steps per period are needed to accurately resolve a given frequency. This would mean that 320 time steps are needed in the  $2\pi$  time interval in order to provide adequate resolution for both the low and high frequencies, as is evidenced by the results shown in Figure 6.

The third condition on the maximum time step one may take is the CFL condition imposed on the numerical scheme for integrating the governing equations of the system. For a flow system, this could be very severe for low reduced frequencies with an explicit time marching scheme and a fine computational grid. Reference<sup>12</sup> provides estimates on the time steps needed for the Euler and Navier-Stokes equations by an explicit scheme versus an implicit scheme. For an implicit scheme the maximum time step is governed by accuracy of the time discretization regardless of the CFL number. For a 2nd order implicit scheme, 32 time steps per period is adequate as discussed in the above paragraph. With an explicit scheme, however, time steps of the order of thousands may be needed for each period for the Euler and Navier-Stokes equations depending on the spatial grid size. Since an implicit scheme is used in solving both the aerodynamic system and the linear model system in this paper, the CFL number condition is of no concern. Therefore, 32 time steps are used in one period of the highest frequency component in all of our computations.

The FIM method originated from the idea of selected frequencies of interest by looking only at the power spectrum. Obviously, the computation of the response can not be accurate when the input signal strength goes to zero because numerical noise would overwhelm the computation in such a case. The filtered impulse function (2) seeks to bias the signal strength near several selected frequencies so that the numerical computation will give better accuracies near these frequencies of interest. In practice, however, it is found in this study that no noticeable gains are made over the original impulse function for either the model system or the 2D Isogai wing modal. It appears that the efficiency and accuracy of the indicial method depend predominantly on the numerical integration of the dynamic systems. The crucial conditions for accu-

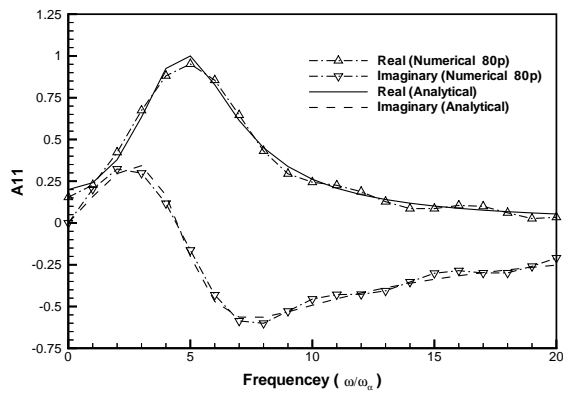


**Fig. 7** Calculated frequency response of the model system by using the IM input with 80 time steps

racy are the length of time integration and the time steps used as discussed in the above paragraphs to guarantee the resolution for both the low and high frequencies as long as the power spectrum of the input signal is not too close to zero.

The advantage of an indicial method is to combine inputs of all frequencies into one single signal so that one execution of the flow code is enough to deduce the response of the system over a range of frequencies. Consequently, it appears that the key is to guarantee a uniform power spectrum of the input signal and adequate computational accuracy in calculating the time domain response over a given bandwidth.

The above discussions seem to suggest that there is no way to escape the requirements of the  $2\pi$  minimum total length of time and a minimum time step size due to accuracy of the integration scheme when the lowest and highest frequencies of interest are blended into one single signal. However, it is noticed from Figures 1, 2, and 3 that the responses of the system decay to zero after the initial disturbance. This suggests that one may truncate the actual computation when the response becomes small enough and pad the solution with zero thereafter. It should be noticed that this is not equivalent to doing Fourier transform directly on the truncated interval since that would reduce the low frequency resolution. In order to verify this idea, computations of only 80 time steps of the originally 320 time steps are performed over the  $2\pi$  period. The solution at the rest of the 240 time steps are padded with zero. The frequency responses calculated in this manner are shown in Figures 7, 9, and 8 along with the exact solution for the IM, FIM, and FIM2 input functions, respectively. Comparisons with the exact solution shown in Figure 7 indicate noticeable but perhaps acceptable errors for the IM input function.

The results calculated by the FIM function shown in Figure 9, however, indicate large errors. This is because the system response has not decayed enough after the first 80 time steps as can be seen from Figure

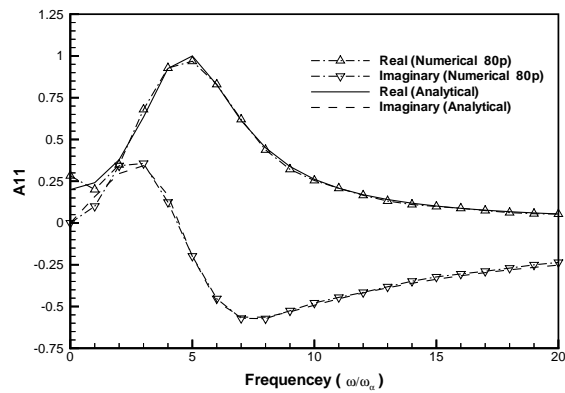


**Fig. 8** Calculated frequency response of the model system by using the FIM2 input with 80 time steps

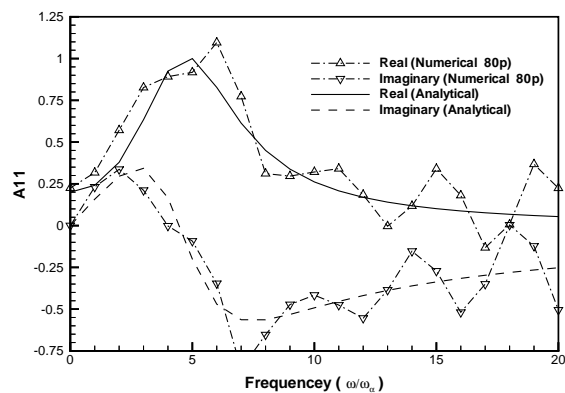


**Fig. 9** Calculated frequency response of the model system by using the FIM input with 80 time steps

2 (dashed line). By increasing the value of  $a$  in Equation (2), one can shorten the duration of the initial disturbance. However, it is found that the response of the system still persists several periods after the input signal vanishes. This is because the large  $a$  value increases the low frequency contents of the input signal and the low frequency response of the system must exhibit itself over a long time. This feature exists also in the response to the original impulse signal since its power spectrum is large near the zero frequency point.

Figure 8 shows the result with the FIM2 input function also by using only 80 time steps in the same manner as described above. Clearly, the numerical result agrees very well with the analytic solution. Examination of the system response shown in Figures 3 indicates that the system response to this FIM2 function dies out faster than those to the IM and FIM functions. It is this fast decay that makes it possible to stop the calculation earlier without degrading accuracy. The fast decay of the system response is due to the reduced low frequency component of the FIM2 function as shown in the power spectrum of Figure

4. The reduced power near  $\omega = 0$  does not significantly affect the accuracy for the low frequency waves as long as the signal strength is not too close to zero. As mentioned earlier, the signal strength for this FIM2 function can be increased by increasing the off-set of  $t_c$  from  $\pi$ . For problems where low frequency responses are not important, one can simply set  $t_c = \pi$  in the FIM2 function and discard the solution at  $\omega = 0$ .

The filtered impulse function in the form of Equation (2) does not seem to perform better than the other two. The constant  $a$  in Equation (2) also has a large effect on the accuracy of the computation. Too large an  $a$  gives sharp peaks and make the signal resemble more the original impulse function with a very large  $W$ . Too small an  $a$ , however, not only unnecessarily weakens the signal strength for frequencies away from the selected frequencies, but also renders the signal persist over a long time. This means that one has to perform the calculations over several periods before an accurate frequency response can be obtained.

Next, the IM, FIM and FIM2 functions are used to solve the Isogai wing model by using the full Euler flow solver. The qualitative behaviors of the three functions found in computation for the model dynamics system still stand for the 2D aerodynamic system. For clarity, only the results with the IM and FIM2 methods are shown here. Figure 10 shows the calculated generalized aerodynamic force coefficient  $A_{11}$  for the Isogai wing model by using the IM and FIM2 inputs with 320 time steps. Clearly, they overlap each other almost perfectly. Therefore, they would be considered as being the 'exact solution' for this case. Figures 11 and 12 show the calculated generalized aerodynamic force coefficient  $A_{11}$  and  $A_{12}$ , respectively, by using the IM and FIM2 inputs with only 64 time steps in the manner described earlier. For comparison purposes, the results by the FIM2 method with 320 time steps are also shown. It can be seen that the FIM2 solutions with 64 time steps are indistinguishable from those with 320 points, whereas the solution with the IM function still shows significant deviations. Figure 13 shows the time history of the generalized aerodynamic forces to the IM and FIM2 inputs. The faster decay of the responses to the FIM2 input supports that accuracy can be retained by the FIM2 function with fewer time steps than by the IM function.

Finally, the computed generalized aerodynamic force coefficients calculated by the FIM2 functions are fed into a standard V-g method to determine the flutter boundary for the Isogai wing model. Figure 14 shows the calculated flutter boundary as compared to that calculated by direct CFD-CSD simulation in References.<sup>3</sup> Except for the solution at  $M = 0.9$ , the results by the indicial method agree well with those by direct simulations. It is not clear yet to the authors why the result at  $M = 0.9$  is very different from those by the direct simulations.

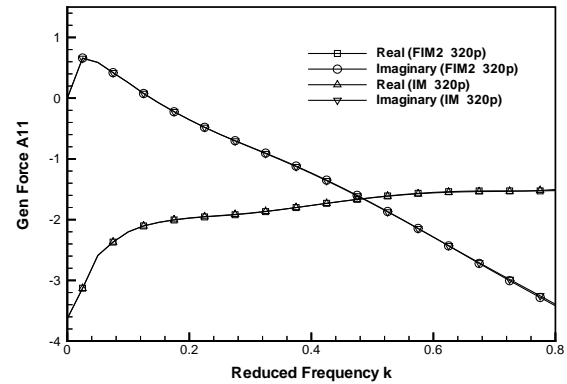


Fig. 10 Calculated generalized aerodynamic force coefficient  $A_{11}$  for the Isogai wing model by using the IM and FIM inputs with 320 time steps

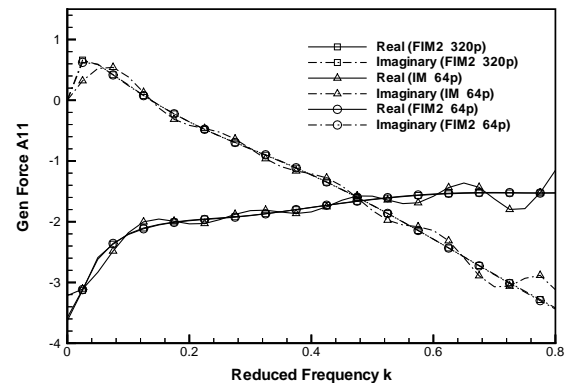


Fig. 11 Calculated generalized aerodynamic force coefficient  $A_{11}$  for the Isogai wing model by using the IM and FIM inputs with 64 time steps

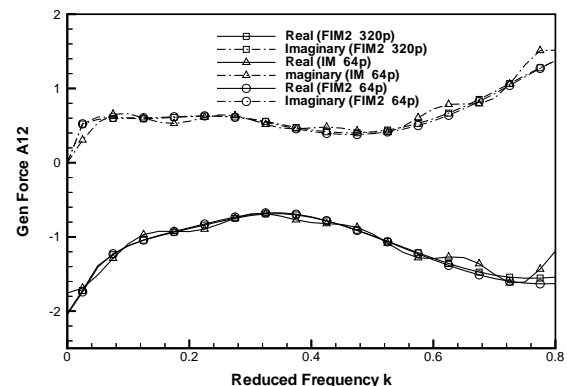


Fig. 12 Calculated generalized aerodynamic force coefficient  $A_{12}$  for the Isogai wing model by using the IM and FIM inputs with 64 time steps

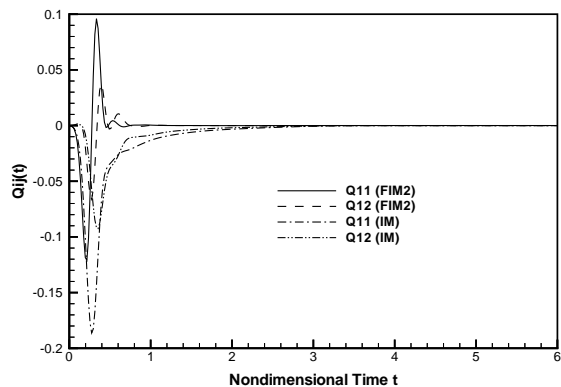


Fig. 13 Comparison of responses of the Isogai wing model to the IM and the FIM2 inputs

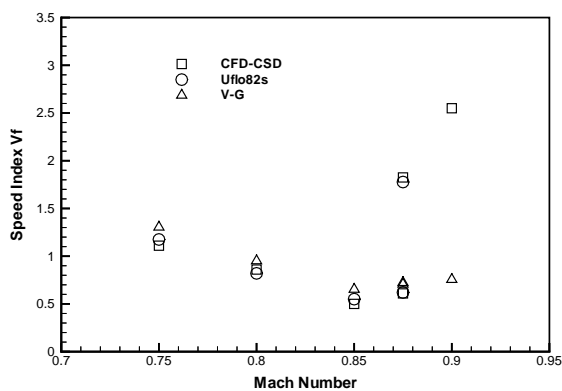


Fig. 14 Comparison of flutter boundary of the Isogai wing calculated by the V-g method based on the indicial response calculated by the FIM2 input and that calculated by direct CFD-CSD simulation in Reference<sup>3</sup>

## VII. Conclusions

In calculating the response of a system to a given input function by using a numerical time marching algorithm, the minimum time interval over which computations must be performed must be at least one period of the lowest frequency component of interest, while the maximum allowable time step size must guarantee at least 32 time steps within one period of the highest frequency component of interest for a 2nd order time marching scheme. A new strategy for calculating the frequency response is proposed in which the time integration of the flow system is stopped when the response approaches zero and the solution for the rest of the period is padded with zero.

Three input signals are tested for use in an indicial method for calculating the frequency response of a model dynamic system and an aerodynamic system. A new input function called the FIM2 function properly distributes energy over a given bandwidth while avoiding sharp corner and peaks that may cause

numerical difficulties for a CFD code. Only the maximum frequency of interest needs to be specified for this function. It automatically adjust its width and decaying rate for proper resolution of the specified frequency range. The  $t_c$  parameter in the description of the function can be adjusted to reduce or increase the signal strength at zero frequency. Lower frequency contents at zero make the response decay faster so that computational time can be shortened. The new FIM2 input function is used to predict flutter by using an unsteady Euler/Navier-Stokes CFD code. It needs less computational time for the same accuracy compared to the conventional impulse function.

## References

- <sup>1</sup>Robinson, B. A., Batina, J. T., and Yang, H. T. Y., "Aeroelastic Analysis of Wings Using the Euler Equations with a Deforming Mesh," *Journal of Aircraft*, Vol. 28, No. 11, Nov.-Dec. 1991, pp. 778-788.
- <sup>2</sup>Alonso, J. J. and Jameson, A., "Fully-Implicit Time-Marching Aeroelastic Solutions," AIAA Paper 94-0056, Jan. 1994.
- <sup>3</sup>Liu, F., Cai, J., Zhu, Y., Wong, A. S. F., and Tsai, H.-M., "Calculation of Wing Flutter by a Coupled CFD-CSD Method," AIAA Paper 00-0907, Jan. 2000.
- <sup>4</sup>Tobak, M., "On the Use of Indicial Function Concept in the Analysis of Unsteady Motions of Wings and Wing-Tail Combinations," NACA Report 1188, 1954.
- <sup>5</sup>Ballhaus, W. F. and Goojrian, P. M., "Computation of Unsteady Transonic Flows by the Indical Method," *AIAA Journal*, Vol. 16, No. 2, Feb. 1978, pp. 117-124.
- <sup>6</sup>Seidel, D., Bennet, R., and Ricketts, R., "Some Recent Applications of XTRAN3S," AIAA Paper 83-1811, July 1983.
- <sup>7</sup>Chen, P. C., "Private Communications," 1996.
- <sup>8</sup>Isogai, K., "On the Transonic-Dip Mechanism of flutter of a Sweptback Wing," *AIAA Journal*, Vol. 17, No. 7, 1979, pp. 793-795.
- <sup>9</sup>Isogai, K., "On the Transonic-Dip Mechanism of flutter of a Sweptback Wing: Part II," *AIAA Journal*, Vol. 19, No. 7, 1981, pp. 1240-1242.
- <sup>10</sup>Wong, A. S. F., Tsai, H.-M., Cai, J., Zhu, Y., and Liu, F., "Unsteady Flow Calculations with a Multi-Block Moving Mesh Algorithm," AIAA Paper 00-1002, Jan. 2000.
- <sup>11</sup>Jameson, A., "Time dependent calculations using multigrid, with applications to unsteady flows past airfoils and wings," AIAA Paper 91-1596, June 1991, 10th AIAA Computational Fluid Dynamics Conference.
- <sup>12</sup>Liu, F. and Ji, S., "Unsteady Flow Calculations with a Multigrid Navier-Stokes Method," *AIAA Journal*, Vol. 34, No. 10, Oct. 1996, pp. 2047-2053.